Transport and structural study of $Tl_2Ba_2CuO_{6+\delta}$ single crystals prepared by the KCl flux method

Takashi Manako, Yoshimi Kubo, and Yuichi Shimakawa
Fundamental Research Laboratories, NEC Corporation, 34, Miyukigaoka, Tsukuba 305, Japan
(Received 27 April 1992)

$Tl_2Ba_2CuO_{6+\delta}$ single crystals are prepared by a KCl flux method. Transport properties and crystal structures are investigated for the samples with various T_c's. The result of structural analysis indicates that the change of T_c is caused by the overdoping of the hole carrier through excess oxygen located between double Tl-O sheets. The out-of-plane resistivity ρ_c is larger than for $YBa_2Cu_3O_7$, but smaller than for $Bi_2Sr_2CaCu_2O_8$. Temperature dependences of ρ_c are metallic for both overdoped nonsuperconducting and 75-K superconducting samples. The temperature dependence of in-plane resistivity ρ_{ab} changes from $\sim T^2$ to $\sim T^1$ with increasing T_c. The Hall coefficient R_H exhibits a characteristic maximum at about 100 K for all samples. However, inverse Hall mobility $\mu_H^{-1}(=\rho/R_H)$ always shows clear T^2 dependence regardless of the T_c values, which suggests that the scattering rate of this material has $\sim T^2$ dependence, just as in an ordinary Fermi liquid, and that the carrier concentration actually changes like that observed in $n_H(=1/R_He)$.

I. INTRODUCTION

High-T_c superconductors have highly anisotropic layered structures with two-dimensional CuO_2 sheets, so single-crystal studies are needed to elucidate the intrinsic in-plane and out-of-plane properties. Single-crystal samples of good quality and sufficient size have been obtained for $(La_{1-x}Sr_x)_2CuO_{4-\delta}$ (La 2:1:4),[1,2] $YBa_2Cu_3O_{7-\delta}$ (Y 1:2:3),[3-5] and $Bi_2Sr_2CaCu_2O_{8+\delta}$ (Bi 2:2:1:2),[6,7] and their physical properties have been examined by various probes. Although these single-crystal samples have various carrier concentrations, only La 2:1:4 can be overdoped to the level of a normal metal. However, the random potential due to Sr^{2+} substitution for La^{3+} in La 2:1:4 may have some undesirable effects on the properties at high doping levels. It is strongly emphasized, however, that the research approach from the overdoped metallic side is very important because the high-T_c superconductivity occurs in an intermediate region between an antiferromagnetic insulator and an overdoped nonsuperconducting normal metal.

Previously, we have demonstrated that $Tl_2Ba_2CuO_{6+\delta}$ (Tl 2:2:0:1) undergoes a well-defined superconductor-to-normal-metal transition when hole carriers are overdoped with excess oxygen.[8,9] In this material, the temperature dependence of resistivity shows a gradual change from $\sim T^1$ to $\sim T^2$ with increasing doping. The Hall coefficient R_H also gradually decreases with doping. Thus, no singularity has been observed in either the crystal structures or the physical properties at the superconductor-metal phase boundary. This result contrasts sharply with that for La 2:1:4, in which the Hall coefficient R_H changes sign from positive to negative at the phase boundary.[10] This remarkable difference between La 2:1:4 and Tl 2:2:0:1 may be caused by the difference in the manner of carrier doping. Namely, La 2:1:4 is doped by Sr^{2+} substitution for La^{3+}, which will produce significant randomness in the CuO_2 plane, whereas Tl 2:2:0:1 is doped by the incorporation of excess oxygen atoms at interstitial sites between double TlO layers located far from the CuO_2 plane. Thus, Tl 2:2:0:1 seems to be the best prototype for investigating the intrinsic properties of the overdoped region.

Recently, we have prepared Tl 2:2:0:1 single crystals by a KCl flux method and revealed that the T_c values of single-crystal samples are also changed reversibly by annealing in the same manner as for polycrystal samples.[11,12] This paper describes the preparation of the single crystals and their refined crystal structures for both superconducting and nonsuperconducting samples. The Hall coefficient and the anisotropy of resistivity are also reported.

II. EXPERIMENT

A. Sample preparation

Single-crystal samples were prepared by a slow cooling method using a KCl flux. At first, a single-phase Tl 2:2:0:1 powder was prepared from Tl_2O_3, BaO, and CuO by a conventional solid-state reaction. Then the Tl 2:2:0:1 powder and KCl flux were mixed with the ratio of [Tl 2:2:0:1]/[KCl]=1–10 wt %, and charged into a gold crucible (20 mm diameter and 25 mm high). The crucible was covered up with gold foil because both KCl and thallium are very volatile. The mixture was then melted at 920 °C for 3 h and cooled to 750 °C at 1–10 °C/h. The temperature gradient essential for nucleation was provided by blowing oxygen gas on a small area of the crucible wall. The grown single crystals were easily collected without flux sticking to the crystal surface by dissolving the KCl flux in water.

The single crystals were thin and platelike, grown in the a-b plane, with a typical size of $2\times2\times0.01$ mm^3. The a-b plane was fairly flat but small growth steps were observed on the surface. The homogeneity of supercon-

ductivity in the samples of various T_c's was checked by measuring the Meissner effect. The as-grown crystal samples had a T_c of about 40 K. After annealing in oxygen at 350 °C for 10 h, their T_c decrease to ≤ 10 K. Subsequent annealing in Ar at 400–500 °C for 10 h produced sharp transitions up to 75 K. These changes in T_c were perfectly reversible and all samples showed a sharp, single transition at T_c. The Meissner fraction (the ratio of the Meissner signal to perfect diamagnetism) for the sample with T_c of 50 K was about 33%. These facts indicate that the superconductivity of these crystals is fairly homogeneous and bulklike.

B. Measurements

The crystal structure was analyzed with a RIGAKU RASA5R four-circle x-ray diffractometer using Mo $K\alpha$ radiation. Single-crystal samples were cut into $50\times50\times10$ μm^3 pieces and mounted at the top of a capillary. The computer program TEXSAN was used for least-squares refinement of the structure parameters. An absorption correction based on Ψ scan data was applied in the refinement. In-plane resistivity ρ_{ab} and the Hall coefficient R_H were measured by the van der Pauw method under a magnetic field of up to 6 T. The out-of-plane resistivity ρ_c and ρ_{ab} were measured by the Montgomery method. The samples for transport measurement were obtained by cutting the crystals into pieces of uniform thickness. The electrical contacts were made through four small gold pads formed by dc sputtering. Gold wires of 30 μm diameter were connected to the gold pads by silver paste. A subsequent annealing at 400 °C for 5 h in flowing oxygen was needed to reduce the contact resistance to less than 1 Ω. In both measurements, the electrodes must be placed on the crystal edge. In particular, in the Montgomery method, they must be placed at the vertices of the rectangular crystal. To satisfy this requirement, the crystal edges were cleaved after making gold pads near the crystal edges. The conventional four-probe method was also used for the ρ_{ab} measurements to verify the van der Pauw and Montgomery calculations.

III. RESULTS AND DISCUSSION

A. Structure

Crystal structures of the samples with T_c's of 0 and 40 K were analyzed on the basis of tetragonal space group of $I4/mmm$ (No. 139). The refined results are listed in Tables I and II. The site notation in this paper, except for the O(4) site, follows that of a powder neutron-diffraction study of Tl 2:2:0:1.[13] The O(4) atom is assigned a 4*d* site instead of the 8*g* site used in the previous work because the *R* factors have not improved by adopting the 8*g* site for the O(4) atom. Unfortunately, the poor x-ray-scattering ability of the oxygen atom results in quite large uncertainties in its structural parameters. However, the existence of excess oxygen at the O(4) site is above suspicion because the R_{wp}'s are lowered from 5.21 to 5.20 % for the 40-K sample and from 5.32% to 5.29 % for the 0-K sample by taking the O(4) atom into account in crystal structure refinements. Consequently, we only made qualitative discussions about oxygen. Anisotropic thermal parameters are given for Tl, Ba, Cu, O(1), and O(2). In the final fitting cycle, the occupation factors *g* for these atoms are fixed to 1 because they are very close to 1. The thermal parameter of the O(3) atom on the TlO layers is rather large when it is located at an ideal 4*e* site (0,0,*z*), suggesting the static displacement of this atom. Thus, the O(3) atom is located on four equivalent sites (16*n*) close to an ideal 4*e* site with *g* of 0.25.

As T_c increases from 0 to 40 K, the occupancy of the interstitial oxygen O(4) site between double Tl-O sheets decreases from 0.084 to 0.028, which corresponds to the decrease in excess oxygen per formula unit from 0.168 to 0.056. Although these values are somewhat larger or smaller than those determined previously by neutron diffraction for polycrystal samples[13] and have quite large uncertainties, this decease in excess oxygen with increasing T_c is quite consistent with the previous result. Positional and thermal parameters for other atoms are almost identical to both neutron-diffraction[13,14] and single-crystal x-ray-diffraction[15] results.

As the oxygen content decreases, both the *c*-axis length and the bond length between Cu and apical oxygen O(2)

TABLE I. Crystallographic data for the Tl 2:2:0:1 single crystal with T_c of 40 K. *g* is the occupation factor. The U_{ij}'s are anisotropic thermal parameters and B_{eq} is the equivalent isotropic thermal parameter. The isotropic thermal parameter of the O(4) site was fixed at 1.0. The numbers in the parentheses are estimated standard deviations in the last decimal place. $a_0=3.867$ Å, $c_0=23.210$ Å. Note that $R_{wp}=5.20\%$ and $R=4.36\%$. The composition determined by these data is $Tl_2Ba_2CuO_{6.056}$.

Atom	Site	*x*	*y*	*z*	B_{eq} (Å^2)	U_{11} (Å^2)	U_{22} (Å^2)	U_{33} (Å^2)	*g*
Tl	4*e*	0	0	0.297 18(8)	1.467	0.023 8(7)	0.023 8(7)	0.008 0(7)	1
Ba	4*e*	0	0	0.083 4(1)	0.624	0.005 7(7)	0.005 7(7)	0.012(1)	1
Cu	2*b*	0	0	0.5	0.544	0.002 3(17)	0.002 3(17)	0.016(4)	1
O(1)	4*c*	0	0.5	0	0.754	0.011(13)	0.008(10)	0.010(11)	1
O(2)	4*e*	0	0	0.384 3(14)	1.589	0.017(10)	0.017(10)	0.027(19)	1
O(3)	16*n*	0	0.104(13)	0.209 7(16)	0.728				0.25
O(4)	4*d*	0	0.5	0.25	1.000				0.028(64)

TABLE II. Same as for Table I, but for the Tl 2:2:0:1 single crystal with a T_c of 0 K: $a_0 = 3.864$ Å and $c_0 = 23.165$ Å. Note that $R_{wp} = 5.29\%$ and $R = 4.46\%$. The composition determined by these data is $Tl_2B_2CuO_{6.164}$.

Atom	Site	x	y	z	B_{eq} (Å^2)	U_{11} (Å^2)	U_{22} (Å^2)	U_{33} (Å^2)	g
Tl	4e	0	0	0.296 99(9)	1.552	0.026 1(8)	0.026 1(8)	0.006 5(6)	1
Ba	4e	0	0	0.084 1(1)	0.740	0.007 0(7)	0.007 0(7)	0.014(1)	1
Cu	2b	0	0	0.5	0.732	0.004 5(18)	0.004 5(18)	0.018(4)	1
O(1)	4c	0	0.5	0	1.075	0.04 (11)	0.018 (14)	0.017(12)	1
O(2)	4e	0	0	0.384 3(14)	1.845	0.024 (11)	0.024(11)	0.022(18)	1
O(3)	16n	0	0.109 (16)	0.209 7(16)	2.000				0.25
O(4)	4d	0	0.5	0.25	1.000				0.084(68)

increase by about 0.2%, whereas the distance between the Ba ion and the CuO_2 sheet decreases by 0.6%. These changes of interatomic distances are understood in terms of a simple electrostatic picture. Since the incorporation of excess oxygen provides hole carriers in the CuO_2 plane, it will be charged more positively. Therefore, the positive Ba ions are repelled from it whereas negative O ions are attracted to it. In addition, it is noted that both the thermal parameter and the static displacement from the ideal 4e site for O(3) increase with excess oxygen. This suggests that some relaxation in Tl-O sheets is caused by the incorporation of oxygen at the interstitial site. All these results agree well with the previous powder neutron-diffraction study.[13]

B. Out-of-plane resistivity

Figure 1 shows the Montgomery resistances, R_1 and R_2, for the samples with T_c's of 0 and 75 K. The inset is the contact configurations used for these measurements. R_1 represents the ratio of the voltage cross 1,2 and the current through 3,4, while the R_2 is that of the voltage cross 1,3 and the current through 2,4. The large values of R_1 and R_2 ($> 10^{-3}$ Ω) as well as the small ratio of R_1/R_2 (< 30) assure the sufficient accuracy in the Montgomery calculation, in which R_1 and R_2 are transformed into the resistivity components ρ_{ab} and ρ_c.[16,17]

Figure 2 shows the temperature dependence of the out-of-plane resistivity ρ_c for these two samples together with those for other materials. The anisotropy ρ_{ab}/ρ_c versus temperature is shown in Fig. 3. The anisotropy increases as temperature decreases, but the difference between two samples is not large at room temperature. This contrasts sharply with the result for underdoped La 2:1:4 and Y 1:2:3, in which the anisotropy drastically changes with a small change in the doping level. At room temperature, both ρ_c ($\sim 10^{-1}$ Ω cm) and anisotropy ρ_c/ρ_{ab} ($6-8\times 10^2$) are larger than for Y 1:2:3 but smaller than for Bi 2:2:1:2, while ρ_{ab} is similar ($\sim 10^{-4}$ Ω cm) for all materials. The temperature dependence of ρ_c shows a metallic behavior even in the 75-K superconducting sample.

Previously, Ito *et al.* have pointed out, on the basis of the Mott-Ioffe-Regel limit, that $d\rho_c/dT$ will be negative when ρ_c is larger than approximately 10^{-2} Ω cm.[18] However, the ρ_c values in the present work exceed this limit by an order of magnitude. Moreover, the temperature dependence of ρ_c for Bi 2:2:1:2 also shows metallic behavior above 100 K, in spite of the very large ρ_c value of ~ 10 Ω cm. Therefore, it seems difficult to explain the

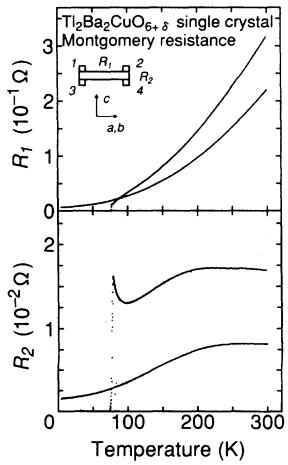

FIG. 1. Montgomery resistances measured for the samples with T_c's of 0 and 75 K. The inset is a schematic of the contact configuration.

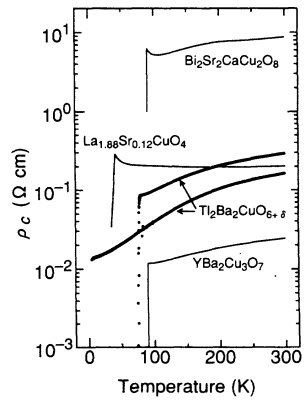

FIG. 2. Temperature dependencies of ρ_c plotted vs temperature for $Tl_2B_2CuO_{6+\delta}$, $Bi_2Sr_2CaCu_2O_8$ (after Ref. 7), $La_{1.88}Sr_{0.12}CuO_4$ (after Ref. 2), and $YBa_2Cu_3O_7$ (after Ref. 4).

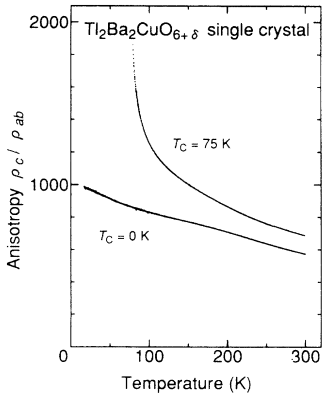

FIG. 3. Anisotropy of resistivity (ρ_c/ρ_{ab}) plotted vs temperature for $Tl_2Ba_2CuO_{6+\delta}$ with T_c's of 0 and 75 K.

out-of-plane conduction in terms of the ordinary Mott-Ioffe-Regel model. Finally, considering the large variation of ρ_c among the high-T_c cuprates, it is suggested that ρ_c does not play an important role in high-T_c superconductivity, which seems to bespeak the strong two-dimensional (2D) nature of these materials.

C. In-plane resistivity and the Hall coefficient

The in-plane resistivity ρ_{ab} was measured by the van der Pauw method and the Montgomery method as well as the conventional four-probe method. Figure 4 shows the temperature dependent ρ_{ab} for samples of different T_c's measured by these three methods. The lower T_c values

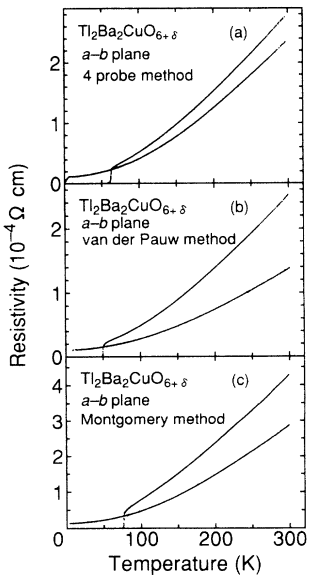

FIG. 4. Temperature dependencies of in-plane resistivity measured by (a) a conventional four-probe method, (b) a van der Pauw method, and (c) a Montgomery method for $Tl_2Ba_2CuO_{6+\delta}$ single-crystal samples with low-T_c (≤ 10 K) and high-T_c (≥ 50 K) values.

($T_c \leq 10$ K) are obtained by annealing the samples in an oxygen atmosphere at 350 °C for 10 h, after making the electrical contacts; the higher-T_c values ($T_c \geq 50$ K) are achieved by annealing the low-T_c samples in argon at 400–500 °C without removing the electrodes. The ρ_{ab} values at room temperature for the low-T_c samples range from 135 to 286 $\mu\Omega$ cm. This variation in ρ_{ab} seems to be due to the error in measuring sample dimensions as well as the difference in sample quality. However, it is noted that the temperature dependencies of ρ_{ab} for the low-T_c samples are quite similar ($\sim T^2$). Moreover, as T_c increases, the magnitude of ρ_{ab} increases and the temperature dependence changes from $\sim T^2$ to $\sim T^1$. Such variation in the temperature dependence of resistivity is very similar to that observed for polycrystal samples.[9] To analyze the temperature dependence of resistivity we first made a power-law fit expressed as

$$\rho = \rho_0 + AT^{\alpha} , \tag{1}$$

where ρ_0 is the residual resistance. This expression provides fairly good fits for all the ρ-T curves in Fig. 1. The obtained exponent α is plotted versus T_c in Fig. 5. It is clear that the α values change systematically with T_c for all samples, which shows that the temperature dependence of ρ_{ab} obtained from these three methods is identical, although the absolute values differ by a factor of ~ 2.

The R_H values for samples with T_c values of 10 and 50 K are plotted versus temperature in Fig. 6(a). For the low-T_c sample, R_H is about 1.0×10^{-3} cm^3C^{-1} and shows a broad maximum at about 100 K. For the high-T_c sample, the R_H values become larger and the maximum at about 100 K becomes more pronounced. This tendency is seen more clearly in the temperature dependence of the Hall number $n_H (=1/eR_H)$ as shown in Fig. 6(b). Obviously, the n_H of both samples decrease linearly as temperature decreases from 300 to ~ 150 K, and show an upturn below 100 K. These results agree well with those for polycrystal samples.[9] Therefore, the transport

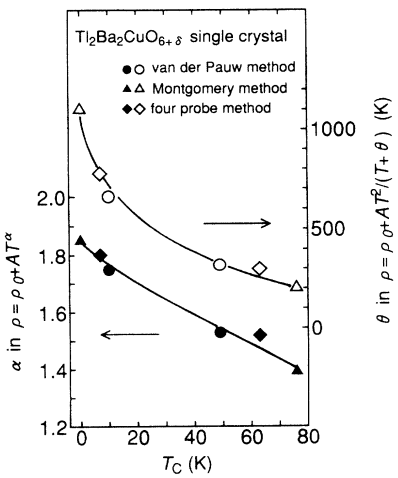

FIG. 5. Exponent α in $\rho=\rho_0+AT^{\alpha}$ and characteristic temperature θ in $\rho=\rho_0+AT^2/(T+\theta)$ are plotted vs T_c for the in-plane resistivity data of Fig. 4.

properties of polycrystal samples mainly reflect the in-plane properties, although the resistivity is rather enhanced in polycrystal samples. This seems to be due to the large anisotropy of this material. The temperature dependencies of the Hall mobility μ_H $(=R_H/\rho)$ are shown in Fig. 6(c). The μ_H value increases as temperature decreases, but the difference between the two samples is rather small. These results are also similar to those for polycrystal samples, except that the values for single crystals are about five times larger.

Looking more closely at the temperature dependence of ρ_{ab}, although the power-law expression (1) can be fitted for the entire temperature range, there are significant deviations in the high-temperature region (>200 K). Moreover, the residual resistivity ρ_0 becomes negative for some high-T_c samples. These facts suggest that the exponent α changes with temperature. Figure 7 shows the

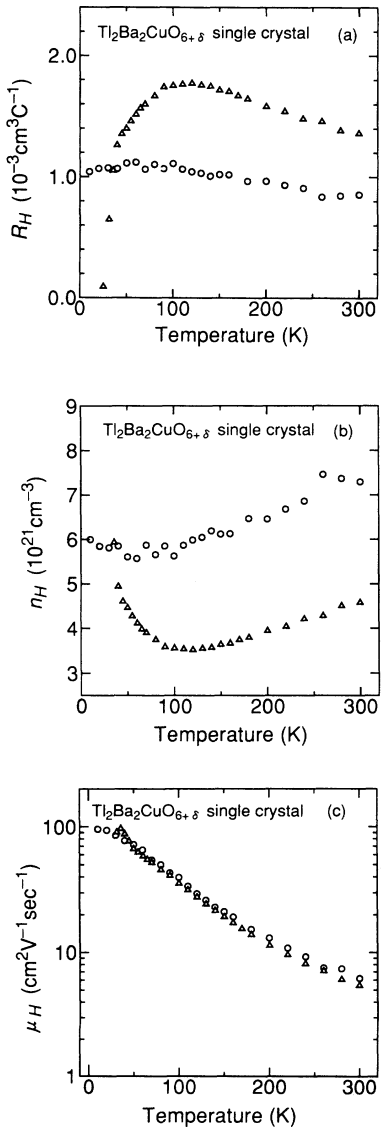

FIG. 6. Temperature dependencies of the (a) Hall coefficient, (b) Hall number, and (c) Hall mobility for samples with T_c's of 10 K (circles) and 50 K (triangles).

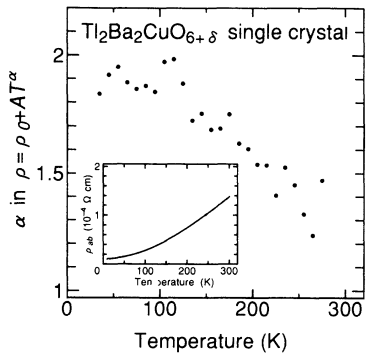

FIG. 7. Temperature dependence of the local exponent α for the normal metallic sample of Fig. 4(b), calculated in the temperature range of 50 K around each temperature. The inset is the raw data used for this calculation.

"local" α values for the low-T_c sample of the van der Pauw method, which are obtained by fitting in a temperature range of 50 K around each temperature. It is clear that the exponent α decreases from ~ 2.0 to ~ 1.2 as temperature increases. A similar tendency is observed for the high-T_c sample. Thus, the temperature dependence of ρ_{ab} is not easily expressed by a single exponential term throughout the wide temperature range.

Next, we tried to fit the data using a two-carrier model, in which parallel conduction by two types of hole carriers with different scattering rates of $\sim T^2$ and $\sim T^1$ is assumed. In that case, the temperature dependence of resistivity will change from $\sim T^1$ at high temperatures to $\sim T^2$ at low temperatures, just as in the result of Fig. 7. Since the total conductivity is the sum of the two contributions, i.e.,

$$\sigma \sim n_1 A/T + n_2 B/T^2 , \tag{2}$$

where n_1 and n_2 are the carrier concentrations for the two carriers, the resistivity is expressed as

$$\rho = \rho_0 + CT^2/(T+\theta) , \tag{3}$$

where $C = 1/n_1 A$, and $\theta = n_2 B/n_1 A$ is the crossover temperature between low-temperature $\sim T^2$ and high-temperature $\sim T^1$ dependencies. This expression gives very good fits over the entire temperature region. Moreover, the ρ_0 values are scarcely changed by the change in T_c. Refined θ values for the data in Fig. 4 are plotted versus T_c in Fig. 5. It is noted that the θ value systematically decreases with increasing T_c just like the exponent α in the power-law fit. Since θ is determined by the ratio of n_2/n_1, the change of the exponent α in the power-law expression (1) is interpreted as a change in the ratio of the two carriers. However, this method is inconsistent with the temperature dependence of the Hall coefficient. In this model, the Hall coefficient is expressed as

$$R_H = (T^2/n_1 + \theta^2/n_2)/(T+\theta)^2 . \tag{4}$$

Expression (4) has a minimum at a characteristic temperature, B/A, whereas the observed Hall coefficients show a maximum at about 100 K. Therefore, the above two-carrier model seems to be unacceptable even though it

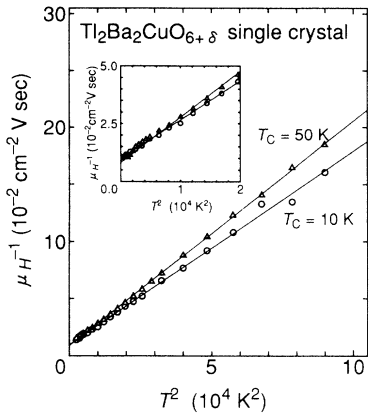

FIG. 8. Inverse Hall mobility (μ_H^{-1}) plotted vs T^2 for $Tl_2Ba_2CuO_{6+\delta}$ with T_c's of 10 K (circles) and 50 K (triangles).

can explain the temperature dependence of ρ_{ab}.

Recently, we proposed another interpretation, in which the carrier concentration actually changes with temperature, as shown in the temperature dependence of the Hall coefficient.[19] Although both resistivity and the Hall coefficient show rather complicated temperature dependencies, the inverse Hall mobility $\mu_H^{-1}=\rho/R_H$ shows clear T^2 dependence for both low-T_c and high-T_c samples (Fig. 8). It is specially notable that the anomaly (minimum) of n_H at $\sim$100 K completely disappears in the μ_H^{-1} plot. Such a temperature dependence of μ_H^{-1}, or $\cot\theta_H=\mu_H^{-1}B$, where B is the applied field, is also observed for Y 1:2:3 and its Zn-doped version.[20] Anderson has explained these results by distinguishing the transverse (Hall) relaxation time τ_H from the transport relaxation time τ_{tr}.[21] According to this theory, the transverse scattering rate τ_H^{-1} and the transport scattering rate τ_{tr}^{-1} have temperature dependencies of $\sim T^2$ and $\sim T^1$, respectively. However, it seems to be difficult to explain the gradual change in τ_{tr}^{-1} from T^2 to T^1 dependencies without changing the temperature dependence of τ_H^{-1}. On the contrary, if an isotropic mobility $\mu(=e\tau/m^*)=\mu_H=\mu_{tr}$ is assumed for these materials, the present results mean that μ^{-1} always obeys $\sim T^2$ just as in an ordinary Fermi liquid. In that case, the temperature dependence of R_H is considered to reflect a real change in carrier concentration, namely, $n_H\sim n$, where n is the carrier concentration. Thus, ρ_{ab} will vary with T^2/n_H, which becomes same as expression (3) above 100 K because n_H linearly increases with $\sim(T+\theta)$. Indeed, the θ values obtained from a linear extrapolation of n_H in Fig. 6(b) are 635 and 404 K, which agree well with the values obtained by fits to expression (3) (Fig. 5).

IV. CONCLUSION

$Tl_2Ba_2CuO_{6+\delta}$ single crystals were prepared by a KCl flux method and their crystallographic and electrical properties were investigated. The T_c values were varied from 75 to $\leq$10 K by annealing in Ar or O_2. The superconductivity of the crystals was confirmed to be fairly homogeneous and bulklike. Crystal structure analysis revealed that the excess oxygen is located at interstitial sites between double TlO layers. The out-of-plane resistivity ρ_c was as large as $\sim 10^{-1}$ Ω cm, which is larger than for Y 1:2:3 but smaller than for Bi 2:2:1:2, but temperature dependencies of ρ_c were still metallic. The temperature dependence of in-plane resistivities ρ_{ab} changed from $\sim T^2$ to $\sim T^1$ with increasing T_c, while the Hall coefficient R_H showed a maximum at $\sim$100 K for all samples. However, although ρ and R_H had such a complicated temperature dependence, the inverse Hall mobility $\mu_H^{-1}(=\rho/R_H)$ always showed a clear T^2 dependence over the entire temperature range. These results suggest that the scattering rate always obeys a Fermi-liquid-like T^2 dependence, and that the carrier concentration varies with temperature as observed in the temperature dependence of n_H.

[1] I. Tanaka and H. Kojima, Nature (London) **337**, 21 (1989).
[2] S. Kambe, K. Kitazawa, M. Naito, A. Fukuoka, I. Tanaka, and H. Kojima, Physica C **160**, 35 (1989).
[3] H. Takei, H. Asaoka, Y. Iye, and H. Takeya, Jpn. J. Appl. Phys. **30**, L1102 (1991).
[4] T. A. Friedmann, M. W. Rabin, J. Giapintzakis, J. P. Rice, and D. M. Ginsberg, Phys. Rev. B **42**, 6217 (1990).
[5] J. P. Rice, J. Giapntzakis, D. M. Ginsberg, and J. M. Mochel, Phys. Rev. B **44**, 10 158 (1991).
[6] L. Forro, D. Mandrus, C. Kendziora, L. Mihaly, and R. Reeder, Phys. Rev. B **42**, 8704 (1990).
[7] S. Martin, A. T. Fiory, R. M. Fleming, L. F. Schneemeyer, and J. V. Waszczak, Phys. Rev. Lett. **60**, 2194 (1988).
[8] Y. Shimakawa, Y. Kubo, T. Manako, and H. Igarashi, Phys. Rev. B **40**, 11 400 (1989).
[9] Y. Kubo, Y. Shimakawa, T. Manako, and H. Igarashi, Phys. Rev. B **43**, 7875 (1991).
[10] H. Takagi, T. Ido, S. Ishibashi, M. Uota, S. Uchida, and Y. Tokura, Phys. Rev. B **40**, 2254 (1989).
[11] T. Manako, Y. Shimakawa, Y. Kubo, and H. Igarashi, Physica C **185-189**, 1327 (1991).
[12] T. Manako, Y. Shimakawa, Y. Kubo, and H. Igarashi, Physica C **190**, 62 (1991).
[13] Y. Shimakawa, Y. Kubo, T. Manako, H. Igarashi, F. Izumi, and H. Asano, Phys. Rev. B **42**, 10 165 (1990).
[14] J. B. Parise, C. C. Torardi, M. A. Subramanian, J. Gopalakrishnan, and A. W. Sleight, Physica C **159**, 239 (1989).
[15] C. C. Torardi, M. A. Subramanian, J. C. Calabrese, J. Gopalakrishnan, E. M. McCarron, K. J. Morrissey, T. R. Askew, R. B. Flippen, U. Chowdhry, and A. W. Sleight, Phys. Rev. B **38**, 225 (1988).
[16] H. C. Montgomery, J. Appl. Phys. **42**, 2971 (1971).
[17] B. F. Logan, S. O. Rice, and R. F. Wick, J. Appl. Phys. **42**, 2975 (1971).
[18] T. Ito, H. Takagi, S Ishibashi, T. Ido, and S. Uchida, Nature (London) **350**, 596 (1991).
[19] Y. Kubo and T. Manako, Physica C **197**, 378 (1992).
[20] T. R. Chien, Z. Z. Wang, and N. P. Ong, Phys. Rev. Lett. **67**, 2088 (1991).
[21] P. W. Anderson, Phys. Rev. Lett. **67**, 2092 (1991).